



# Submillisecond Unfolding Kinetics of Apomyoglobin and its pH 4 Intermediate

**Marc Jamin<sup>1</sup>, Syun-Ru Yeh<sup>2</sup>, Denis L. Rousseau<sup>2</sup> and Robert L. Baldwin<sup>1\*</sup>**

<sup>1</sup>Department of Biochemistry  
Stanford University Medical Center, Stanford, CA 94305-5307, USA

<sup>2</sup>Department of Physiology and Biophysics, Albert Einstein College of Medicine, Bronx NY 10461, USA

Submillisecond mixing experiments and tryptophan fluorescence spectroscopy are used to address two questions raised in earlier stopped-flow studies of the folding and unfolding kinetics of sperm whale apomyoglobin. A study of the pH 4 folding intermediate (*I*) revealed, surprisingly, that its folding and unfolding kinetics are measurable and fit the two-state model except for a possible burst phase in unfolding. Submillisecond mixing experiments confirm the unfolding burst phase and show that its properties are consistent with the recently discovered interconversion between two forms of *I*, *Ia* ⇌ *Ib*. In urea-induced unfolding, *Ib* is converted to *Ia* before *Ia* unfolds, and the unfolding kinetics of *Ia* fit the two-state model when the burst phase is assigned to *Ib* → *Ia*. The second question is whether the *Ia*, *Ib* intermediates accumulate transiently when the native protein (*N*) unfolds to the acid unfolded form (*U*). Earlier work showed that *Ia* and *Ib* accumulate when *U* refolds to *N* at pH 6.0 and the results fit the linear folding pathway *U* ⇌ *Ia* ⇌ *Ib* ⇌ *N*. We report here that either or both *Ia* and *Ib* accumulate transiently when *N* unfolds to *U* at pH 2.7 and that the position of the rate-limiting step in the pathway changes between unfolding at pH 2.7 and refolding at pH 6.0. In unfolding as in refolding, we do not detect a fast track that bypasses the *Ia*, *Ib* intermediates.

© 1999 Academic Press

\*Corresponding author

**Keywords:** folding intermediate; apomyoglobin; molten globule; cooperativity; tryptophan fluorescence

## Introduction

The pH 4 equilibrium intermediate (*I*) of apoMb has striking properties which make it a desirable choice for studies of the mechanism of protein folding. First, *I* is formed rapidly in the kinetic process of forming the native apoMb structure at pH 6.0 (Jennings & Wright, 1993), so that detailed characterization of *I* can be made at equilibrium at pH 4 and the results can be used to describe the kinetic folding intermediate at pH 6. Second, the kinetics of folding and unfolding *I* are measurable by stopped-flow methods inside the urea-induced unfolding transition at pH 4.2, 4.5°C, and the kinetics fit the two-state model *I* ⇌ *U* (*U* = unfolded), with one caveat that is discussed below (Jamin & Baldwin, 1996). Third, there are two distinguishable forms of *I*, *Ia* and *Ib*, which coexist in a pH- and urea-dependent equilibrium, and which are

interconvertible with measurable kinetics in the millisecond time range (Jamin & Baldwin, 1998). These earlier kinetic results for the overall refolding reaction of apoMb are consistent with the linear model *U* ⇌ *Ia* ⇌ *Ib* ⇌ *N* (*N* = native) in which both *Ia* and *Ib* are on-pathway intermediates.

We ask first if the *U* ⇌ *Ia* reaction inside the urea-induced unfolding transition (pH 4.2) is truly two-state when monitored by Trp fluorescence. Jamin & Baldwin (1996) found that the kinetics fit the two-state model except for a possible burst phase (missing amplitude) in the unfolding reaction. Because they could monitor only the last half of the kinetic reaction, both in unfolding and refolding, their observation of a burst phase in unfolding was tentative. If the submillisecond mixing experiments, which we report here, confirm the presence of a burst phase, and if the burst phase is demonstrated to be part of the unfolding reaction of *I*, this would mean that its unfolding is not completely cooperative. When the kinetics of the *U* ⇌ *I* transition were first reported, the existence of two

E-mail address of the corresponding author:  
rbaldwin@cmgm.stanford.edu

forms of *I* was not known. Later, Jamin & Baldwin (1998) reported that, at low urea concentrations (below 1 M), *Ib* is converted to *Ia* and the unfolding transition of *I*, which occurs above 1 M urea, is in fact the unfolding transition of *Ia*. In unfolding experiments with *I*, it is now necessary to take account of the *Ib* = *Ia* reaction.

Our second aim involves submillisecond mixing experiments on the unfolding of *N* at pH 2.7, in the absence of urea. The aim is to test whether *Ia* and *Ib* accumulate transiently when *N* unfolds to *U*, as predicted by the model derived from the refolding experiments, *U* = *Ia* = *Ib* = *N*, when the rates of the various steps are extrapolated down to pH 2.7. The accumulation of these intermediates during the process of unfolding of *N* would bear out the existence of a defined macroscopic pathway. Some simulations suggest that the refolding process should proceed more rapidly by bypassing folding intermediates which are predicted to act as kinetic traps in folding (see Dill & Chan, 1997; Wolynes, 1997). A basic prediction is that molecules that fold by pathways that avoid populated intermediates will be observed to fold on a "fast track". A previous study of apoMb refolding at pH 6.0 found that the intermediates *Ia*, *Ib* accumulate transiently and there is no evidence for a fast track that bypasses *Ia*, *Ib* (Jamin & Baldwin, 1998). The formation of *N* was monitored by a sensitive and specific assay, its unfolding rate: this assay can detect a small amount of *N* in the presence of larger amounts of folding intermediates (Kiehaber, 1995). We ask here if the *Ia*, *Ib* intermediates accumulate transiently when *N* unfolds to *U* at pH 2.7. It is straightforward to answer this question with the equipment used here because the fluorescence emission maxima of *Ia*, *Ib* occur at wavelengths quite different from those of *N* and *U*. Both the disappearance of *N* and the formation of *U* occur with measurable kinetics under the conditions used here, when observed with submillisecond mixing.

Although there are two distinguishable intermediates, *Ia* and *Ib*, they are not resolved from each other in some types of experiments and we use the collective term *I* to refer to the mixture of *Ia*, *Ib* when they are not resolved.

## Results

### Folding and unfolding kinetics of *I* at pH 4.2

The mechanism of folding and unfolding of the pH 4 folding intermediate, inside the urea-induced unfolding transition, is studied here with a continuous-flow rapid mixing apparatus which operates at a fixed temperature of 20 °C (dead-time ~200 μs) (Takahashi *et al.*, 1997). The kinetics are monitored by recording the Trp fluorescence spectrum at different time points. The folding intermediate *I* has a fluorescence intensity higher than those of *U* and *N*, and the fluorescence changes for *U* to *Ia*, *Ia* to *Ib* and *Ib* to *N* have been used pre-

viously to monitor the folding kinetics of *U* to *Ia* and *U* to *N* (Jamin & Baldwin, 1996, 1998). The Trp fluorescence spectrum shifts when the Trp side-chain becomes accessible to the aqueous solvent, and the position of the emission maximum is a sensitive indicator of Trp burial. It provides a more reliable signal for identifying large conformational changes than the fluorescence intensity.

In preliminary experiments, the fluorescence spectra of the starting materials for the refolding and unfolding of *I* were measured, namely *U* at pH 4.2 in 4.0 M urea and *I* at pH 4.2 in 0 M urea. At pH 4.2, where both *Ia* and *Ib* are present, the emission maximum of *I* is at 353 nm, whereas the maximum occurs at 359 nm in the spectrum of the unfolded protein (*U*). Under the same conditions (4.5 °C, in 2 mM sodium citrate, 30 mM NaCl, pH 4.2), the equilibrium unfolding transition of *I* takes place above 1 M urea, with a midpoint near 1.9 M (Jamin & Baldwin, 1996). The folding and unfolding kinetics measured here at various urea concentrations inside the urea-induced unfolding transition reveal changes in both the intensity and the shape of the fluorescence spectrum. Figure 1(a) shows the unfolding kinetics at 2.2 M urea monitored by the fluorescence intensity at 340 nm and by the red-shift of the emission maximum. Up to 70% of the reaction is observed; the measured part follows an exponential time course with decreasing intensity and the emission maximum shifts from 354 nm to 358 nm. Extrapolation to time zero indicates that at least one additional reaction occurs during the mixing: it involves a small red-shift of the emission maximum (~1 nm) and a rise in fluorescence intensity. This burst phase amplitude increases slightly when the urea concentration increases (data not shown). The refolding kinetics measured inside the transition region also follow an exponential time course. Figure 1(b) shows the refolding kinetics measured at 1.5 M urea. In contrast to the unfolding kinetics, however, there is no burst phase: the variations in both intensity and blue-shift of the emission spectrum account for the entire changes expected from the initial and final equilibrium spectra.

The observed rate constant ( $1/\tau$ ) increases with increasing [urea] in the unfolding experiments, increases with decreasing [urea] in the refolding experiments and proceeds through a minimum in the transition region. Similar values of the observed rate constant are found in the folding and unfolding directions. A plot of  $\ln(1/\tau)$  versus final [urea] in Figure 1(c) is fitted to equation (2), which is derived for a two-state model (see Materials and Methods) when there is a linear dependence of  $\ln(k)$  on [urea] (Chen *et al.*, 1989). Because the data at 20 °C are limited, the kinetic *m* values determined previously at 4.5 °C are used in fitting. The rate constants for folding and unfolding, obtained by extrapolation to 0 M urea, are:  $k_{12}(\text{H}_2\text{O}) = 21,700 \text{ s}^{-1}$  and  $k_{21}(\text{H}_2\text{O}) = 220 \text{ s}^{-1}$ . The free energy change for unfolding at 0 M urea, 20 °C, calculated from the

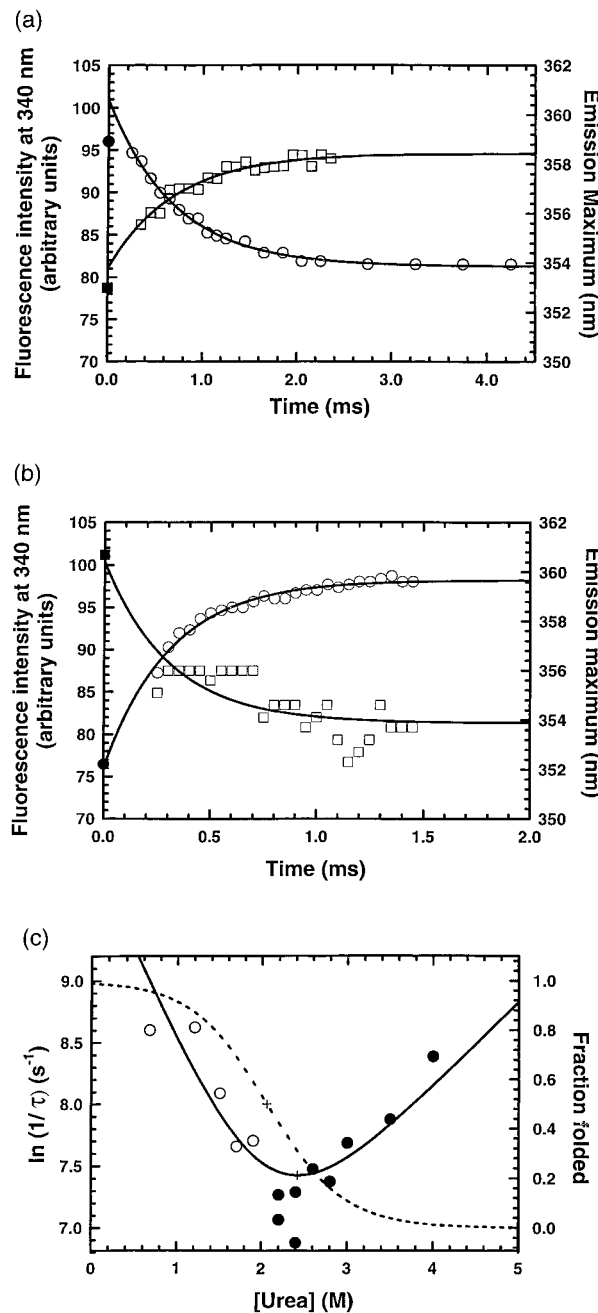


**Figure 1.** Urea-induced unfolding and refolding kinetics of the pH 4 intermediate. Variation of the fluorescence intensity at 340 nm ( $\circ$ ) and of the position of the emission maximum ( $\square$ ) are shown as a function of time for unfolding at 2.2 M urea (a) and for refolding at 1.5 M urea (b). The fluorescence intensity and position of the emission maximum measured in the initial conditions are shown by filled symbols ( $\bullet$ ,  $\blacksquare$ ). Conditions: 2 mM sodium citrate, 30 mM NaCl, pH 4.2, 20°C; initial protein concentration is 20  $\mu$ M in 0 M urea for unfolding and in 4 M urea for refolding. The fluorescence values are normalized so that the value at pH 4.2, 0 M urea, in (a) is 96 (as in Figure 3 of Jamin & Baldwin, 1998). In each Figure, the kinetics monitored by fluorescence intensity at 340 nm was fitted to a three-parameter exponential equation,  $F = F_{\text{final}} - A \times \exp(-k \times r)$ , in which the amplitude ( $A$ ), the apparent rate constant ( $k$ ) and the fluorescence intensity at equilibrium ( $F_{\text{final}}$ ) are adjustable

forward and backward rate constants ( $\Delta G_{\text{unf}} = 2.7$  kcal/mol), is slightly higher than the value obtained previously at 4.5° ( $\Delta G_{\text{unf}} = 2.4$  kcal/mol), as expected if the intermediate is slightly more stable near 20°C because it exhibits cold denaturation (Nishii *et al.*, 1994). The equilibrium transition curve in Figure 1(c) is calculated from the folding and unfolding rate constants at each urea concentration. The midpoint of the equilibrium transition appears shifted towards lower [urea] as compared to the point of the  $V$  in the kinetic plot where  $1/\tau$  is minimal. This shift is predicted by the two-state model because the value of  $[\text{urea}]_{(1/\tau)_{\min}}$  depends on the ratio of the kinetic  $m$  values (equation (3)). The midpoint of the equilibrium transition ( $C_m$ ) occurs where the microscopic rate for folding equals that for unfolding.

### pH dependence of the folding and unfolding kinetics at 4.5°C

At low salt conditions, the pH-induced unfolding transition of native apoMb shows two well separated steps between pH 6 and 2 (Griko *et al.*, 1988; Barrick *et al.*, 1993). An intermediate, actually an equilibrium mixture of two distinct forms, *Ia* and *Ib*, is populated near pH 4 (Jamin & Baldwin, 1998). The overall folding and unfolding kinetics of apoMb at 4.5°C and various final pH values are measured here in pH-jump experiments monitored by Trp fluorescence. Figure 2 shows the pH dependence of the observed rate constants (Figure 2(a)) and kinetic amplitudes (Figures 2(b), (c)) for the various kinetic phases observed in both folding and unfolding directions.

parameters. The kinetics of the emission maximum change was fitted to a two-parameter exponential equation in which the observed rate constant  $k$  was obtained from the fit of the fluorescence intensity. The lines in (a) are drawn using the following parameters. Fluorescence intensity:  $A = -19.7$ ,  $k = 1.43 \text{ s}^{-1}$ ,  $F_{\text{final}} = 81.3$ . Emission maximum:  $A = 4.6$ ,  $k = 1.43 \text{ s}^{-1}$  (fixed),  $\lambda_{\text{max}}(\text{final}) = 358.4$ . The lines in (b) are drawn using the following parameters. Fluorescence intensity:  $A = 22.2$ ,  $k = 3.24 \text{ s}^{-1}$ ,  $F_{\text{final}} = 98.2$ . Emission maximum:  $A = -6.5$ ,  $k = 3.24 \text{ s}^{-1}$  (fixed),  $\lambda_{\text{max}}(\text{final}) = 353.9$ . (c) The reciprocal of the relaxation time ( $1/\tau$ ) versus urea molarity for refolding from 4 M urea ( $\circ$ ) and unfolding from 0 M urea ( $\bullet$ ). The line shows a fit of the data to equation (2) for a two-state model with  $k_{12(\text{H}_2\text{O})} = 21,700 \text{ s}^{-1}$ ,  $m_{12} = -0.9 \text{ kcal.mol}^{-1} \text{ M}^{-1}$ ,  $k_{21(\text{H}_2\text{O})} = 220 \text{ s}^{-1}$ ,  $m_{21} = 0.4 \text{ kcal.mol}^{-1} \text{ M}^{-1}$ . The broken line shows the equilibrium transition curve calculated from these parameters assuming a two-state model. The symbol + shows the midpoint of the equilibrium transition ( $C_m = 2.06 \text{ M}$ ) and the  $[\text{urea}]_{\min}$  (2.42 M).

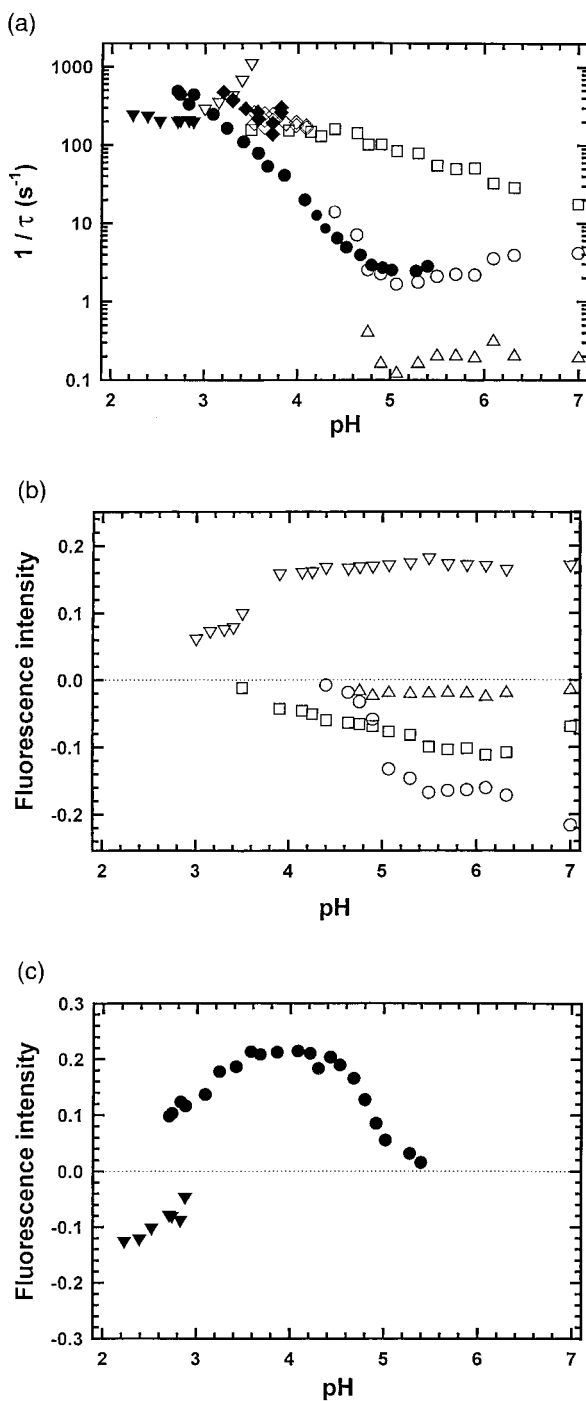


**Figure 2.** pH dependences of the folding and unfolding kinetics at 4.5°C. Conditions: 2 mM sodium citrate, 30 mM NaCl, initial protein concentration 20 μM. The starting material for unfolding is *N* at pH 6.0 and for refolding it is *U* at pH 2.2 (a) Apparent rate constants. Filled symbols are for the unfolding kinetics ( $\blacktriangledown$ ,  $\blacklozenge$ ,  $\bullet$ ), and open symbols are for refolding kinetics ( $\triangledown$ ,  $\square$ ,  $\diamond$ ,  $\circ$ ,  $\triangle$ ). The diamonds ( $\lozenge$ ,  $\blacklozenge$ ) represent the data obtained previously by pH jump between pH 3.1 and 4.1 (Jamin & Baldwin, 1998). The triangles ( $\triangle$ ) show the apparent rate constant for the formation of *N* from the slow dissociation of a dimeric species (Jamin & Baldwin, 1998). (b) and (c) Amplitudes of the different phases measured in the refolding (b) and unfolding directions (c). The symbols are the same as in (a). Between pH 3.0 and 3.4, the amplitude of the first kinetic phase of

### Refolding kinetics

For the refolding experiments, the starting material is *U* at pH 2.2 and the kinetic behavior changes with pH. (a) When the refolding reaction is measured at a pH above 4.5, three phases plus a burst phase are observed. These kinetic phases were assigned earlier at pH 6.0 (Jamin & Baldwin, 1998) and, by continuity, they are now assigned throughout the pH range from pH 3.4 to 7.0. The  $U \rightleftharpoons I_a$  reaction occurs during the mixing time and gives rise to the burst phase change. The  $I_a \rightleftharpoons I_b$  reaction is the first measurable phase: its observed rate varies from  $150 \text{ s}^{-1}$  at pH 3.4 to  $30 \text{ s}^{-1}$  at pH 6.0. Native apoMb *N* is formed in each of the last two kinetic phases. The slowest phase, whose amplitude depends on the protein concentration, represents the dissociation of a dimeric or oligomeric intermediate. It contributes less than 10% of the native protein formed in these experiments. The rate of forming *N* from monomeric *Ib* at pH 6.0 is  $3.3 \text{ s}^{-1}$ . (b) When refolding is measured at a pH between 3.4 and 4.5, only one phase is observed in addition to the burst phase. The observed rate matches that of the  $I_a \rightleftharpoons I_b$  reaction measured previously between pH 3.1 and 4.1 (Jamin & Baldwin, 1998). The previous data are also shown in Figure 2(a). (c) When refolding is measured below pH 3.4, a single exponential phase with increasing fluorescence intensity is observed. Both the rate and amplitude of this phase increase with pH and the reaction becomes too fast to measure above pH 3.4. We show below that this reaction is  $U \rightleftharpoons I_a$ .

### Unfolding kinetics

For the unfolding experiments, the starting material is *N* at pH 6.0, and the kinetic behavior again changes with pH. (a) When unfolding is measured above pH 3.0, unfolding produces an exponential rise in fluorescence intensity whose amplitude accounts for the entire change expected from the equilibrium transition curve. The rate increases as the pH decreases and, by continuity, it matches the rate of the  $I_b \rightleftharpoons N$  reaction. Near pH 4.0, *Ia* and *Ib* are the end products of the unfolding reaction but, because the  $I_a \rightleftharpoons I_b$  reaction is faster than the  $I_b \rightleftharpoons N$  reaction,  $I_a \rightleftharpoons I_b$  is not detected in the unfolding kinetics. (b) When unfolding is observed below pH 3.0, biphasic kinetics are seen in which a species accumulates transiently whose fluorescence intensity is higher than those of *U* and *N*. Figure 3 (trace 1) shows the

---

refolding ( $\triangledown$ ) is the measured amplitude, whereas above pH 3.4, the same symbol ( $\triangledown$ ) shows the amplitude of the burst phase calculated from the sum of the amplitudes of the other kinetic phases and from the initial and final fluorescence values. The other symbols are as in (a).

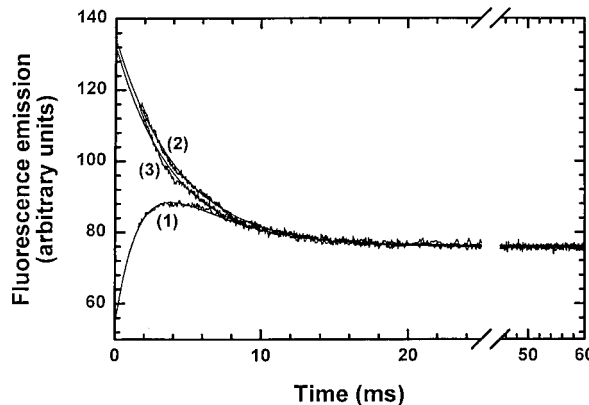


**Figure 3.** Millisecond unfolding kinetics at pH 2.7 measured with a stopped-flow at 4.5°C. Conditions: 2 mM sodium citrate, 30 mM NaCl, initial protein concentration 20  $\mu$ M. The different time traces show the unfolding kinetics starting from different conditions: *N* at pH 6.0 (1) or a mixture of *Ia* and *Ib* at pH 4.2 (2) or 3.5 (3). The kinetic traces are fitted to a single (pH 4.2 and 3.5) or double exponential equation (pH 6.0). The lines are drawn using the following values for the amplitudes, rate constants and final fluorescence intensity: (1) at pH 6.0,  $A_1 = 0.088$ ,  $k_1 = 538 \text{ s}^{-1}$ ,  $A_2 = -0.063$ ,  $k_2 = 240 \text{ s}^{-1}$ ,  $F_{\text{final}} = 0.085$ ; (2) at pH 4.2,  $A_1 = -0.066$ ,  $k_1 = 227 \text{ s}^{-1}$ ,  $F_{\text{final}} = 0.085$ ; (3) at pH 3.5,  $A_1 = -0.063$ ,  $k_1 = 252 \text{ s}^{-1}$ ,  $F_{\text{final}} = 0.086$ .

unfolding kinetics of *N* at pH 2.7; the transient species is formed with an observed rate constant of  $540 \text{ s}^{-1}$  ( $\tau_1 = 1.9 \text{ ms}$ ) and it disappears in the second phase with an observed rate constant of  $240 \text{ s}^{-1}$  ( $\tau_2 = 4.2 \text{ ms}$ ).

#### Transient accumulation of an intermediate when *N* unfolds at pH 2.7

To find out whether the biphasic change of Trp fluorescence at low pH is caused by the accumulation of the folding intermediates *Ia* and *Ib*, the unfolding kinetics at pH 2.7 were observed starting from different initial pH values (Figure 3). When the starting material is *N* at pH 6.0 (trace 1), biphasic kinetics are observed. The ratio of the amplitudes of the fast and slow unfolding phases is independent of protein concentration over the range 5 to 40  $\mu$ M (data not shown), which excludes the formation of a multimeric species as the origin of the biphasic kinetics. When the starting material is a mixture of *Ia* and *Ib* at either pH 4.2 (trace 2) or pH 3.5 (trace 3), only the second phase ( $1/\tau = 220\text{-}250 \text{ s}^{-1}$ ) is observed, showing that the fast rise in fluorescence intensity when *N* is present initially is caused by the disappearance of *N*. The kinetic amplitude and the observed rate of the slow kinetic phase are independent of the initial conditions, suggesting that  $\text{Ia} \rightleftharpoons \text{Ib}$  equilibration is rapid at pH 2.7 and the slow step is  $\text{Ia} \rightleftharpoons \text{U}$ . This deduction follows because the initial ratio  $[\text{Ib}]/[\text{Ia}]$  varies with pH between 4.2 and 3.5.

Clear evidence for the transient accumulation of *I* during the unfolding of *N* at pH 2.7 is provided by time-resolved Trp-fluorescence spectroscopy studies. The fluorescence spectrum of *I* has a greater intensity than those of *U* and *N*, but, more importantly, its  $\lambda_{\text{max}}$  is about halfway between those of *U* and *N*. The emission spectra of the starting material (*N* at pH 6.0) and of the final product at pH 2.7 (a mixture of *U* and *I*) are shown in Figure 4(a), together with the spectra taken at different times of the reaction. The fluorescence spectrum of the transient species, recorded after 300  $\mu$ s of unfolding, has  $\lambda_{\text{max}} = 353 \text{ nm}$ , almost halfway between those of the final product at pH 2.7 ( $\lambda_{\text{max}} = 356 \text{ nm}$ ) and *N* at pH 6.0 ( $\lambda_{\text{max}} = 348 \text{ nm}$ ); its spectrum is compared in Figure 4(b) with the spectrum of the pH 4.2 equilibrium intermediate. The  $\lambda_{\text{max}}$  of the fully acid-unfolded protein at pH 2.2 is at 359 nm (data not shown). Figure 5(a) shows the biphasic variation of the fluorescence intensity at a single wavelength. The kinetic trace is fitted to a double exponential equation. Figure 5(b) shows that each phase involves a red-shift of the emission maximum.

No additional faster or slower reaction, involving either a significant change in fluorescence intensity or a red-shift of the spectrum, is detected in the unfolding kinetics. The kinetic trace in Figure 5(a) extrapolates at time zero to a fluorescence value close to that of the native protein, and the spectrum recorded after 4.1 ms of unfolding can almost be superimposed on the spectrum recorded at equilibrium at pH 2.7 (Figure 4(a)).

## Discussion

### Two-state formation of *Ia*

We obtained measurements in the submillisecond time range of the kinetics of folding and unfolding of the pH 4 intermediate of apoMb at 20°C. These new data provide a more reliable assignment of the kinetics and confirm the highly cooperative character of the  $\text{U} \rightleftharpoons \text{Ia}$  transition (Jamin & Baldwin, 1996). First, in refolding the shift of  $\lambda_{\text{max}}$  occurs during the measurable part of the kinetics, and in unfolding the largest part of the shift also occurs in the measured part of the kinetics. The refolding results show that there is no early intermediate with a different fluorescence spectrum formed in the mixing time. Sperm whale myoglobin has two Trp residues, which are both in the A helix and are buried in the hydrophobic interface zone between the A, G and H helices. Trp → Phe single mutants show that each Trp residue is partially buried in the pH 4 intermediate *I* (M.J., M.S. Kay and R.L.B., unpublished results), and each Trp residue helps to stabilize *I* (Kay & Baldwin, 1996). The present results, together with earlier ones, strongly argue that the  $\text{U} \rightleftharpoons \text{Ia}$  reaction is the cooperative assembly of *Ia*. Second, the rapid mixer we utilize here has extended the time window into the submillisecond domain. It

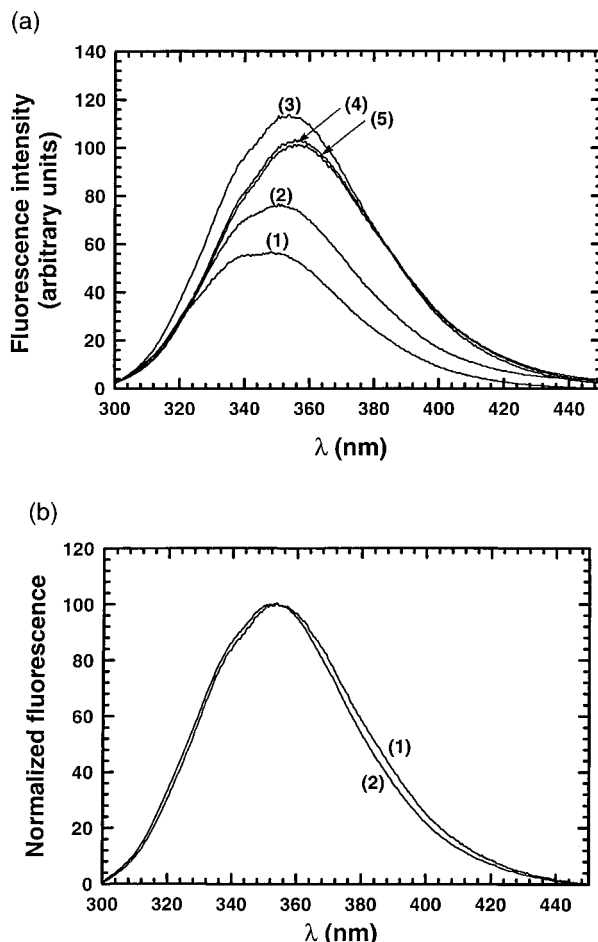


**Figure 4.** Fluorescence emission spectra. (a) Emission spectra of *N* at pH 6.0 (1), of the equilibrium mixture of *U* and *I* at pH 2.7 (5) and after different times during the course of the unfolding of *N* at pH 2.7: 125  $\mu$ s (2), 300  $\mu$ s (3) and 4.1 ms (4). The fluorescence intensity is normalized so that the value at 340 nm, pH 6.0 is 55 in order to match our previous data (Figure 1, Jamin & Baldwin, 1998). (b) Comparison of the spectrum taken after 300  $\mu$ s of unfolding (1) with the spectrum of the pH 4.2 equilibrium intermediate (2). The spectra are normalized so that the value at 450 nm is 0 and the value at 350 nm is 100.

improves the accuracy with which the kinetic amplitude is determined and confirms the existence of a burst phase in the unfolding kinetics (Jamin & Baldwin, 1996). A simple explanation for this missing amplitude can now be proposed, based on the discovery that two forms of the intermediate, *Ia* and *Ib*, coexist at equilibrium between 0 and 1 M urea (Jamin & Baldwin, 1998). *Ib* has a lower fluorescence intensity than *Ia* and is converted rapidly to *Ia* with increasing urea concentration (Jamin & Baldwin, 1998). The kinetics of the *Ib*  $\rightarrow$  *Ia* reaction are measurable at 4.5°C in the pre-transition region, but become too fast to measure by stopped-flow mixing above 1 M urea. When the kinetics of the urea-induced unfolding of

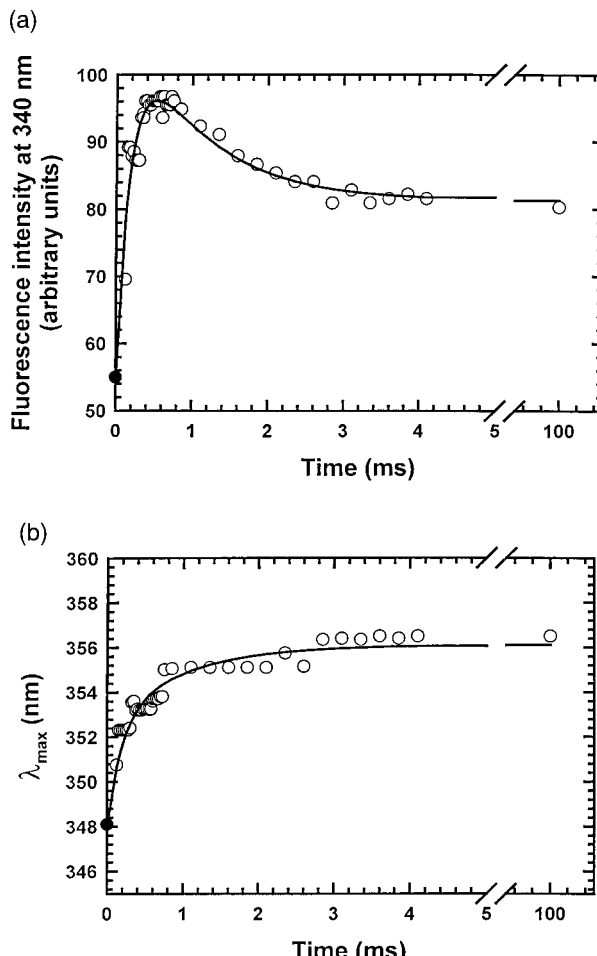


**Figure 5.** Submillisecond unfolding kinetics at pH 2.7 measured with a continuous-flow rapid mixer at 20°C. Conditions: 2 mM sodium citrate, 30 mM NaCl, initial protein concentration 12  $\mu$ M, at pH 6.0. Variation of the fluorescence intensity at 340 nm (○, a) and of the position of the emission maximum (○, b) are shown as a function of time for unfolding at pH 2.7 (a) Fluorescence intensity at 340 nm. The filled circle (●) shows the fluorescence intensity at 340 nm of the native protein at pH 6.0. The fluorescence intensity is normalized so that the initial value at pH 6.0 is 55, according to our previous data (Figure 1, Jamin & Baldwin, 1998). On this normalized scale, the measured value at equilibrium at pH 2.7 is about 82, in good agreement with the value obtained here at the end of the unfolding kinetics. The kinetic trace is fitted to a double exponential equation. The line is drawn using the following values for the amplitudes, rate constants and final fluorescence intensity:  $A_1 = -58.9$ ,  $k_1 = 5200 \text{ s}^{-1}$ ,  $A_2 = 32.0$ ,  $k_2 = 1030 \text{ s}^{-1}$  and  $F_{\text{final}} = 81.3$ . (b) Emission maximum. The filled circle (●) shows the position of the emission maximum of the native protein at pH 6.0. The line represents a fit to a double exponential equation in which the rate constants are fixed to  $k_1 = 5200 \text{ s}^{-1}$  and  $k_2 = 1030 \text{ s}^{-1}$ .

*Ia* are measured at 20°C, only a small rise in fluorescence intensity and a small red-shift of the emission maximum occur within the mixing time, in

agreement with the changes predicted for the  $Ib \rightleftharpoons Ia$  reaction in these conditions.

The kinetics of the  $U \rightleftharpoons Ia$  reaction measured earlier at 4.5 °C (Jamin & Baldwin, 1996, 1998) and here at 20 °C, satisfy several tests showing that it is a two-state reaction when monitored by Trp fluorescence. (1) The measurable part of the folding and unfolding kinetics follows a single exponential time course. The amplitude of the refolding kinetics accounts for the entire change expected from the equilibrium transition curve, and the missing amplitude observed in the unfolding kinetics is explained by the rapid  $Ib \rightarrow Ia$  reaction. (2) The dependence of the observed rate constant on [urea], measured in both folding and unfolding directions, fits the two-state model (equation (2)) and is consistent with the equilibrium transition curve. (3) The  $m$  value and equilibrium constant extrapolated to 0 M urea are similar when calculated either from the kinetic data or from the equilibrium transition curve. Another test for detecting the presence of a kinetic intermediate remains to be made: namely, to compare the kinetics monitored by probes of secondary and tertiary structure.

Two other tests for a two-state  $U \rightleftharpoons Ia$  reaction have been made which confirm the highly cooperative nature of the reaction. First, the equilibrium unfolding curve measured by probes of secondary structure (far-UV CD) and tertiary structure (Trp fluorescence) are superimposable when the proper baseline corrections are made (Kay & Baldwin, 1996). Second, helix-destabilizing mutations (substitution of a Gly or Pro residue) made at solvent-exposed positions in the A and G helices destabilize the entire folding intermediate, and not only the helix in which the substitution is made (Luo *et al.*, 1997). The latter experiments also show, however, that two-state folding of  $Ia$  is a fragile property, easily disturbed by destabilizing mutations.

### ***I* accumulates transiently when *N* unfolds at pH 2.7**

The transient accumulation of  $I$  when  $N$  unfolds at low pH is predicted from the linear  $U \rightleftharpoons Ia \rightleftharpoons Ib \rightleftharpoons N$  model and extrapolation to low pH of the rates assigned to the different reaction steps at high pH. The rates of the  $Ia \rightleftharpoons Ib$  and  $Ib \rightleftharpoons N$  reactions have been determined throughout the pH range from pH 3.4 to 7.0 (Figure 3 and also Figure 2(b)) of Jamin & Baldwin, 1998). Between pH 3.0 and 3.4, an additional kinetic phase is observed in the refolding direction which does not correspond to any of the kinetic phases measured at higher pH. It is assigned to the  $U \rightleftharpoons Ia$  reaction on the basis of the following properties. (1)  $I$  has a fluorescence intensity higher than those of  $U$  and  $N$ . (2)  $Ia$  has a higher fluorescence intensity and a more red-shifted spectrum than  $Ib$ . (3) The additional phase becomes too fast to measure above pH 3.4, and the  $U \rightleftharpoons Ia$  reaction is known to occur in the stopped-flow mixing time during the

refolding of  $N$  at pH 6 (Jamin & Baldwin, 1998). Extrapolation below pH 3.0 of the rates measured at higher pH values predicts that  $N$  forms  $Ib$  faster than  $Ia$  forms  $U$  and therefore that a mixture of  $Ia$  and  $Ib$  accumulates transiently. The fluorescence spectrum of pure  $Ib$  is unknown, and the fractional amounts of  $Ia$  and  $Ib$  cannot be determined.

The observed rate constant and amplitude of the slow unfolding phase at pH 2.7 are insensitive to the initial pH, indicating that unfolding proceeds through the same kinetic barrier whether it is initiated from  $N$  or from a mixture of  $Ia$  and  $Ib$ . This result argues that the intermediates populated when  $N$  unfolds at pH 2.7 are similar to the intermediates present at equilibrium near pH 4 and to the ones formed transiently when  $U$  refolds to  $N$  at pH 6.0. Finding similar intermediates at varying pH values does not mean that their structures and energetics are unaffected by changing pH, but only that the kinetic barriers separating these species from each other remain the same.

### **Kinetic intermediates in unfolding**

Kinetic intermediates in the unfolding reaction of small proteins are rare but not unknown (see Mücke & Schmid, 1994; Zaidi *et al.*, 1997; Kiehaber *et al.*, 1997; Yeh *et al.*, 1998; Yeh & Rousseau, unpublished results). Three classes of folding reactions may be distinguished, not including kinetically complex folding reactions arising from proline isomerization, heme ligand binding or disulfide bond formation. The first class, which includes apoMb and  $\alpha$ -lactalbumin, shows equilibrium folding intermediates which are stable relative to  $U$  under most conditions and also stable relative to  $N$  under restricted conditions, particularly at acid pH. It is not surprising to find these intermediates well populated in kinetic unfolding and refolding experiments. The second class, which includes ubiquitin (Khorasanizadeh *et al.*, 1996), RNase H (Raschke & Marqusee, 1997), barnase (Dalby *et al.*, 1998) and hen lysozyme (Radford *et al.*, 1992), shows two-state folding reactions at equilibrium but complex kinetics of refolding, indicative of refolding intermediates. Unfolding intermediates are observed much more rarely in this class, possibly because the transition state lies between the intermediate and the native state. A third class of folding reactions, which includes the small proteins C12 (Jackson & Fersht, 1991), CspB (Schindler *et al.*, 1995) and protein L (Scalley *et al.*, 1997), shows no observed kinetic intermediates either in refolding or unfolding. Whether or not the folding mechanism of the third class is intrinsically the same as in the first two classes, with the difference in folding behavior being caused only by the reduced stability of folding intermediates, is still under discussion: see review by Baldwin & Rose (1999).

### Change in rate-limiting step with pH

The change in kinetic behavior between pH 2.7 and 6.0 is not attributable to a change between two pathways that have different intermediates. Instead, our results show directly that the rate-limiting step in the apoMb folding pathway changes with pH. At pH 6.0, the rate-limiting step in refolding is  $Ib \rightleftharpoons N$  (Jamin & Baldwin, 1998), while we show here that the rate-limiting step in unfolding at pH 2.7 is  $Ia \rightleftharpoons U$  (or, more precisely,  $I \rightleftharpoons U$ :  $Ia$  and  $Ib$  are not resolved here). This observation serves as a reminder, in the case of folding reactions without observable intermediates, that the rate-limiting step in unfolding may not be the same as in refolding if, as is usually the case, the unfolding and refolding conditions are quite different. For barstar, a change in conditions actually produces a change from one unfolding pathway to another (Zaidi *et al.*, 1997).

### Interpretation by a funnel model

There is wide agreement among experimentalists that, as predicted by simulations of the folding process, alternative pathways of folding are available and may even be used simultaneously (see the study of hen lysozyme by Kiefhaber (1995) and Wildegger & Kiefhaber (1997), and the study of barstar unfolding by Zaidi *et al.* (1997)). What has been controversial is whether populated intermediates slow down the folding process sufficiently so that the intermediates act as kinetic traps in folding, and the folding process can go faster by bypassing the intermediates (see Dill & Chan, 1997). Our present results show that in unfolding, as in refolding (Jamin & Baldwin, 1998), a fast track cannot be detected. Presumably this means that the energy landscape is so constructed that the folding and unfolding processes efficiently funnel material into the  $Ia$  and  $Ib$  intermediates. It is difficult to construct a formal proof that these intermediates are or are not on-pathway, and we note only that the linear model  $U \rightleftharpoons Ia \rightleftharpoons Ib \rightleftharpoons N$  is the simplest one and our unfolding results, like the earlier refolding results (Jamin & Baldwin, 1998), can be fitted by this model.

A study of the equilibrium stability of  $I$  relative to  $N$  and  $U$ , over a wide range of pH and urea concentrations (Barrick *et al.*, 1993) showed that  $I$  is stable relative to  $U$  from pH 3 to pH 8 (the pH range above 8 was not studied) and the relative stability of  $I$  increases with pH in this range. This is undoubtedly the basic reason why the  $Ia$  and  $Ib$  intermediates are well populated in the kinetics of unfolding and refolding in this pH range.

### Comparison with other studies of apomyoglobin folding intermediates

The study by Jennings & Wright (1993) of the kinetics of the  $U \rightarrow N$  refolding reaction at pH 6.0

used NMR-hydrogen exchange and amide CD as probes of the folding process. Their NMR-hydrogen exchange results allowed detailed structural comparison of the major, rapidly formed kinetic intermediate at pH 6.0 with the equilibrium intermediate at pH 4.2 (Hughson *et al.*, 1990) and showed that these two intermediates are very similar structurally. They did not detect the  $Ia \rightleftharpoons Ib$  reaction, but this is not surprising because it is not detected by CD and it would be difficult to detect by NMR-hydrogen exchange, given the fast rate of the  $Ia \rightleftharpoons Ib$  reaction at pH 6.0 ( $\tau = 30$  ms). Jennings & Wright (1993) also detected by NMR-hydrogen exchange a late kinetic intermediate (one second), in which the B helix becomes fully protected, which was not detected by Trp fluorescence (Jamin & Baldwin, 1998).

It is difficult to correlate our results with the extensive unfolding kinetics of Gilmanshin *et al.* (1998) (see also Callender *et al.*, 1998) for three reasons. First, they used a probe of secondary structure (FTIR) whereas we use Trp fluorescence, which depends in a complex manner on tertiary structure and even serves as a tertiary probe in the  $U \rightleftharpoons Ia$  reaction (see Jamin & Baldwin, 1998) because the two Trp residues of apoMb are partly buried in the hydrophobic helix interface region provided by the A, G and H helices. Second, they study horse heart Mb whereas we study Mb from sperm whale. Although the two proteins are known to show similar folding behavior, they cannot be assumed to be identical. Finally, the  $Ia \rightleftharpoons Ib$  reaction depends sensitively on pH and on anion conditions in the regime where they measured the unfolding kinetics of  $I$ . It will be necessary to monitor unfolding both by Trp fluorescence and by FTIR of the same protein solution in order to sort out these variables. It is plausible, but by no means certain, that their published results can be interpreted in terms of the same unfolding intermediates ( $Ia$ ,  $Ib$ ) that we study here.

## Materials and Methods

All experiments were performed in 2 mM sodium citrate, 30 mM NaCl.

### Protein expression and purification

A synthetic gene for sperm whale myoglobin was expressed and purified as described (Loh *et al.*, 1995). The heme was removed by acid-acetone precipitation (Fanelli *et al.*, 1958). Protein concentrations were determined by absorbance in 6.0 M GdmCl as described (Edelhoch, 1967) using  $\epsilon_{280\text{ nm}} = 15,200\text{ M}^{-1}\text{ cm}^{-1}$  and  $\epsilon_{288\text{ nm}} = 10,800\text{ M}^{-1}\text{ cm}^{-1}$ .

### Fluorescence continuous-flow experiments

Submillisecond mixing and fluorescence measurements were performed using previously described instrumentation (Takahashi *et al.*, 1997). The output at 264 nm from a frequency-doubled argon ion laser (Coherent) was focused on the continuously flowing

sample in the flow cell. The progress of the reaction was monitored by moving the mixer/observation cell assembly relative to the laser focusing point along the flow direction. The scattered light was collected and focused onto the entrance slit of a polychromator (Spex 270 M) where it was dispersed and detected by a charge coupled device camera (Photometrics). The dead time of the mixing apparatus was determined by examining a well-characterized pseudo-first order reaction of *N*-acetyl-trypophanamide (NATA) and *N*-bromosuccinimide (Peterman, 1979). It was found to be 200(±50) µs at the earliest observable point. Folding and unfolding of apoMb was initiated with the continuous-flow mixer by sixfold dilution of a 10 µM protein solution with a buffer. The fluorescence spectrum of the final product was obtained by collecting the sample at the end of the observation cell and by running it through the apparatus a second time without further dilution.

The fluorescence spectra presented here are not corrected for any wavelength dependence of the detection system accounting for the discrepancy in the position of the emission maximum between these data and our previous data, but the same relative shifts of the fluorescence spectrum with solvent conditions are observed.

### Fluorescence stopped-flow experiments

Data were collected on a sequential mixing stopped-flow instrument (model DX.17 MV) from Applied Photophysics. The excitation was at 288 nm and an optical cut-off filter was used to detect the emission. The pathlength of the cell was 2 mm. A stopped-flow dead time of 1.6 ms was determined by measuring the quenching of *N*-acetyl-trypophanamide fluorescence at varying concentrations of *N*-bromo-succinimide (Peterman, 1979). The kinetic traces obtained in the stopped-flow experiments were fitted to single, double and triple exponential equations with the software provided by Applied Photophysics.

### Fit to a two-state model

For the analysis of the curve of  $1/\tau$  versus urea molarity, we use the characteristic equations for a two-state  $U \rightleftharpoons I_a$  model. In a two-state model, the relaxation time is given by the sum of the forward and backward rate constants:

$$\frac{1}{\tau} = k_{12} + k_{21} \quad (1)$$

The rate constants for folding ( $k_{12}$ ) and unfolding ( $k_{21}$ ) are expressed as functions of urea molarity ( $C$ ) using the standard relations (Tanford, 1970; Chen *et al.*, 1989). The apparent rate constant is fitted to the following equation:

$$\frac{1}{\tau} = k_{12(H_2O)} \times \exp(m_{12}C/RT) + k_{21(H_2O)} \times (\exp m_{21}C/RT) \quad (2)$$

where  $k_{12}(H_2O)$  and  $k_{21}(H_2O)$  are the rate constants for folding and unfolding at 0 M urea, respectively, and the coefficients  $m_{12}$  and  $m_{21}$  describe the dependence of these microscopic rates on urea molarity. They are related to the equilibrium  $m$  value by the following relationship:  $m = m_{12} - m_{21}$ . The data shown in Figure 1(c) have been fitted to equation (2) using SigmaPlot (Jandel Scientific, San Rafael, CA, USA). In the V-shaped dependence of the observed rate constant, the lowest value of  $1/\tau$  is

found where the first-order derivative of equation (2) with respect to [urea] is zero, at  $[urea]_{(1/\tau)_{min}}$ , which is given by equation (3):

$$[Urea]_{(\frac{1}{\tau})_{min}} = \ln \frac{\left( \frac{-k_{12}(H_2O) \times m_{12}}{k_{21}(H_2O) \times m_{21}} \right)}{\frac{m_{21} - m_{12}}{RT}} \quad (3)$$

### Acknowledgements

This research was supported by NIH grants to R.L.B. (GM19988) and D.L.R. (GM54806 and GM54812).

### References

- Baldwin, R. L. & Rose, G. D. (1999). Is protein folding hierarchic? Folding intermediates and transition states. *Trends Biochem. Sci.* **24**, 77-83.
- Berrick, D. & Baldwin, R. L. (1993). Three-state analysis of sperm whale apomyoglobin folding. *Biochemistry*, **32**, 3790-3796.
- Callender, R. H., Dyer, R. B., Gilmanshin, R. & Woodruff, W. H. (1998). Fast events in protein folding: the time evolution of primary processes. *Annu. Rev. Phys. Chem.* **49**, 173-202.
- Chen, B., Baase, W. A. & Schellman, J. A. (1989). Low-temperature unfolding of a mutant of phage T4 lysozyme. 2. Kinetic investigations. *Biochemistry*, **27**, 691-699.
- Dalby, P. A., Oliveberg, M. & Fersht, A. R. (1998). Folding intermediates of wild-type and mutants of barnase. I. Use of  $\phi$ -value analysis and  $m$ -values to probe the cooperative nature of the folding pre-equilibrium. *J. Mol. Biol.* **276**, 625-646.
- Dill, K. A. & Chan, H. S. (1997). From Levinthal to pathways to funnels. *Nature Struct. Biol.* **4**, 10-19.
- Edelhoch, H. (1967). Spectroscopic determination of tryptophan and tyrosine in proteins. *Biochemistry*, **6**, 1948-1954.
- Fanelli, A. R., Antonini, E. & Caputo, A. (1958). Studies of the structure of hemoglobin. I. Physicochemical properties of human globin. *Biochim. Biophys. Acta*, **30**, 608-615.
- Gilmanshin, R., Callender, R. H. & Dyer, R. B. (1998). The core of apomyoglobin E-form folds at the diffusion limit. *Nature Struct. Biol.* **5**, 363-364.
- Griko, Y. V., Privalov, P. L., Venyaminov, S. Y. & Kutyshenko, V. P. (1988). Thermodynamic study of the apomyoglobin structure. *J. Mol. Biol.* **202**, 127-138.
- Hughson, F. M., Wright, P. E. & Baldwin, R. L. (1990). Structural characterization of a partly folded apomyoglobin intermediate. *Science*, **249**, 1544-1548.
- Jackson, S. E. & Fersht, A. R. (1991). Folding of chymotrypsin inhibitor 2. 1. Evidence for a two-state transition. *Biochemistry*, **30**, 10428-10435.
- Jamin, M. & Baldwin, R. L. (1996). Refolding and unfolding kinetics of the equilibrium folding intermediate of apolyoglobin. *Nature Struct. Biol.* **3**, 613-618.
- Jamin, M. & Baldwin, R. L. (1998). Two forms of the pH 4 folding intermediate of apomyoglobin. *J. Mol. Biol.* **276**, 491-504.

- Jennings, P. A. & Wright, P. E. (1993). Formation of a molten globule intermediate early in the kinetic folding pathway of apomyoglobin. *Science*, **262**, 892-896.
- Kay, M. S. & Baldwin, R. L. (1996). Packing interactions in the apomyoglobin folding intermediate. *Nature Struct. Biol.* **3**, 439-445.
- Khorasanizadeh, S., Peters, I. D. & Roder, H. (1996). Evidence for a three-state model of protein folding from kinetic analysis of ubiquitin variants with altered core residues. *Nature Struct. Biol.* **3**, 193-205.
- Kieffhaber, T. (1995). Kinetic traps in lysozyme folding. *Proc. Natl Acad. Sci. USA*, **92**, 9029-9033.
- Kieffhaber, T., Bachmann, A., Wildeger, G. & Wagner, C. (1997). Direct measurement of nucleation and growth rates in lysozyme folding. *Biochemistry*, **36**, 5108-5112.
- Loh, S. N., Kay, M. S. & Baldwin, R. L. (1995). Structure and stability of a second molten globule intermediate in the apomyoglobin folding pathway. *Proc. Natl Acad. Sci. USA*, **92**, 5446-5450.
- Luo, Y., Kay, M. S. & Baldwin, R. L. (1997). Cooperativity of folding of the apomyoglobin pH 4 intermediate studied by glycine and proline mutations. *Nature Struct. Biol.* **4**, 925-930.
- Mücke, M. & Schmid, F. X. (1994). A kinetic method to evaluate the two-state character of solvent-induced protein denaturation. *Biochemistry*, **33**, 12930-129?.
- Nishii, I., Kataoka, M., Tokunaka, F. & Goto, Y. (1994). Cold denaturation of the molten globule states of apomyoglobin and a profile for protein folding. *Biochemistry*, **33**, 4903-4909.
- Peterman, B. F. (1979). Measurement of the dead time of a fluorescence stopped-flow instrument. *Anal. Biochem.* **93**, 442-444.
- Radford, S. E., Dobson, C. M. & Evan, P. A. (1992). The folding of hen lysozyme involves partially structured intermediates and multiple pathways. *Nature*, **358**, 302-307.
- Raschke, T. M. & Marqusee, S. (1997). The kinetic folding intermediate of ribonuclease H resembles the acid molten globule and partially unfolded molecules detected under native conditions. *Nature Struct. Biol.* **4**, 298-304.
- Scalley, M. L., Yi, Q., Gu, H., McCormack, A., Yates, J. R., III & Baker, D. (1997). Kinetics of folding of the IgG binding domain of peptostreptococcal protein L. *Biochemistry*, **36**, 3373-3382.
- Schindler, T., Herrler, M., Marahiel, M. A. & Schmid, F. X. (1995). Extremely rapid protein folding in the absence of intermediates. *Nature Struct. Biol.* **8**, 663-673.
- Takahashi, S., Yeh, S.-R., Das, T., Chan, C.-K., Gottfried, D. S. & Rousseau, D. L. (1997). Folding of cytochrome c initiated by submillisecond mixing. *Nature Struct. Biol.* **4**, 44-50.
- Tanford, C. (1970). Protein denaturation. Part C. Theoretical models for the mechanism of denaturation. *Advan. Protein Chem.* **24**, 2-95.
- Wildeger, G. & Kieffhaber, T. (1997). Three-state model for lysozyme folding: triangular folding mechanism with an energetically trapped intermediate. *J. Mol. Biol.* **270**, 294-304.
- Wolynes, P. G. (1997). Folding funnels and energy landscape of larger proteins within the capillarity approximation. *Proc. Natl Acad. Sci. USA*, **94**, 6170-6175.
- Yeh, S.-R., Han, S. & Rousseau, D. L. (1998). Cytochrome c folding and unfolding: a biphasic mechanism. *Acc. Chem. Res.* **31**, 727-736.
- Zaidi, F. N., Nath, U. & Udgaoonkar, J. B. (1997). Multiple intermediates and transition states during protein folding. *Nature Struct. Biol.* **4**, 1016-1024.

Edited by P. E. Wright

(Received 28 May 1999; accepted 26 July 1999)